

RESEARCH ARTICLE

Boesenbergia Pandurata as an Anti-Breast Cancer Agent: Molecular Docking and ADMET Study

Mohammad Rizki Fadhil Pratama^{1,2}, Ersanda Nurma Praditapuspa³, Dini Kesuma⁴, Hadi Poerwono⁵, Tri Widiandani⁵, and Siswandono Siswodihardjo^{5,*}

¹Doctoral Program of Pharmaceutical Science, Faculty of Pharmacy, Universitas Airlangga, Surabaya 60115, Indonesia; ²Department of Pharmacy, Faculty of Health Science, Universitas Muhammadiyah Palangkaraya, Palangka Raya 73111, Indonesia; ³Master Program of Pharmaceutical Science, Faculty of Pharmacy, Universitas Airlangga, Surabaya 60115, Indonesia; ⁴Department of Pharmaceutical Chemistry, Faculty of Pharmacy, Universitas Surabaya, Surabaya 60293, Indonesia; ⁵Department of Pharmaceutical Sciences, Faculty of Pharmacy, Universitas Airlangga, Surabaya 60115, Indonesia

Abstract: Background: *Boesenbergia pandurata* or fingerroot is known to have various pharmacological activities, including anticancer properties. Extracts from these plants are known to inhibit the growth of cancer cells, including breast cancer. Anti-breast cancer activity is significantly influenced by the inhibition of two receptors: ER- α and HER2. However, it is unknown which metabolites of *B. pandurata* play the most crucial role in exerting anticancer activity.

Objective: This study aimed to determine the metabolites of *B. pandurata* with the best potential as ER- α and HER2 inhibitors.

Methods: The method used was molecular docking of several *B. pandurata* metabolites to ER- α and HER2 receptors, followed by an ADMET study of several metabolites with the best docking results.

Results: The docking results showed eight metabolites with the best docking results for the two receptors based on the docking score and ligand-receptor interactions. Of these eight compounds, compounds **11** ((2S)-7,8-dihydro-5-hydroxy-2-methyl-2-(4"-methyl-3"-pentenyl)-8-phenyl-2H,6H-benzo(1,2-b-5,4-b')dipyran-6-one) and **34** (geranyl-2,4-dihydroxy-6-phenethylbenzoate) showed the potential to inhibit both receptors. Both ADMET profiles also showed mixed results; however, there is a possibility of further development.

Conclusion: In conclusion, the metabolites of *B. pandurata*, especially compounds **11** and **34**, can be developed as anti-breast cancer agents by inhibiting ER- α and HER2.

ARTICLE HISTORY

Received: October 27, 2021
Revised: November 08, 2021
Accepted: November 15, 2021

DOI:
10.2174/1570180819666211220111245

Keywords: ADMET, *Boesenbergia pandurata*, breast cancer, docking, ER- α , HER2.

1. INTRODUCTION

The discovery of new drugs to treat cancer has become a hot topic among researchers. Apart from the high mortality rate caused by cancer, the exact cause is still being studied today [1]. The types of cancer that can affect humans are very diverse, and almost all parts of the human body can develop cancer.

This is complicated by the high level of "personalized medicine" in each case, as the same therapy may not work for other people even though they suffer from the same type of cancer [2]. This is exacerbated by mutations in cancer cells, which can cause resistance to current therapies.

Therefore, a new approach to research related to the discovery of cancer drugs is required, and currently, an increase in *in silico* research utilizing various advantages of computational techniques has been observed [3].

The application of computational techniques in discovering new drug compounds makes it more manageable for researchers to predict the correct candidate compounds to continue research in the laboratory [4]. Among them is molecular docking (or simply docking), a simple *in silico* method for predicting the interaction between the test compound and the target receptor. In addition to describing the pharmacodynamic processes between drug molecules and receptors, docking is also used to screen potential compounds against specific target receptors [5].

One source of information to find new potential compounds is to use isolated secondary metabolites from medicinal plants and their identified chemical structures [6].

*Address correspondence to this author at the Department of Pharmaceutical Sciences, Faculty of Pharmacy, Universitas Airlangga, P.O. Box: 60115, Surabaya, Indonesia; Tel: +62-812-3206-328; E-mail: prof.sis@ff.unair.ac.id

Currently, an increase in *in silico* studies to identify bioactive compounds from medicinal plants has been observed, especially during the current pandemic, limiting researchers' access to the laboratory [7]. This strategy has also been applied to exploring novel anticancer compounds, in which bioactive compounds from medicinal plants are often used as lead compounds for various types of cancer cells [8].

One of the most studied types is breast cancer, the most reported type of cancer, with new cases reaching 2.3 million according to GLOBOCAN 2020 [9]. Breast cancer has several causes, including overexpression of certain hormones or receptors, such as estrogen receptor α (ER- α) and human epidermal growth factor receptor 2 (HER2), accounting for approximately 75% and 20% of all reported cases, respectively [1, 10]. The development of inhibitors against two target receptors is one strategy for discovering new breast cancer drugs, including those derived from natural metabolites [11].

Boesenbergia pandurata or fingerroot is a medicinal plant from Indonesia known to have potential activity as an anticancer, including breast cancer [12]. Several marker compounds in *B. pandurata* have been reported to play a role in this anticancer activity, such as panduratin A, which can inhibit sustaining proliferative signaling by downregulating NF- κ B and CDKs [13, 14] and pinostrobin, which can inhibit cell death resistance through downregulating Bcl-2 [15]. Le Bail *et al.* also reported that pinostrobin could inhibit the growth of breast cancer cells through anti-aromatase activity [16]. This result is supported by a study by Jones and Gehler, who reported that pinostrobin could produce a dose-dependent inhibition of cell adhesion, cell spreading, and focal adhesion formation, which is selective for malignant breast cells [17]. In addition, our previous *in silico* study reported that pinostrobin and its derivatives had better potential than the reference compounds, such as ER- α and HER2 inhibitors, which play a role in breast cancer therapy [18]. However, little is known about the potential anticancer activities of other metabolites of *B. pandurata*.

Ventures to explore the potential activity of *B. pandurata* metabolites *in silico* have been carried out previously, as reported by Youn and Jun, who analyzed *B. pandurata* metabolites using the docking method as a BACE1 inhibitor [19]. However, a similar study examining all *B. pandurata* metabolites that have been identified as having anti-breast cancer activity has not been previously reported. Therefore, this study aimed to determine the metabolite of *B. pandurata*, which has the best potential *in silico* as an inhibitor of ER- α and HER2 by molecular docking method. To obtain a more comprehensive prediction, an ADMET study was also conducted to obtain information regarding the pharmacokinetic characteristics of each metabolite along with its safety profile.

2. MATERIALS AND METHODS

2.1. Hardware and Software

The hardware used was the Toshiba Portege Z30-C series Ultrabook with an Intel™ Core i7-6600U@2.6 GHz and Windows 10 Pro operating system. The software used was Chem3D for energy minimization, OpenBabel 3.1.1 for ligand

and receptor format conversion, AutoDockTools 1.5.6 for docking protocol configuration, AutoDock Vina 1.1.2 for the docking process, PyMOL 2.4.1 for docking protocol validation, UCSF Chimera 1.15rc for the preparation of docking results, and Discovery Studio Visualizer 20.1.0.19295 for visualization and observation of docking results. All software used has a free license, except for PyMOL, for which the evaluation version (30-day trial) was used. The ADMET prediction servers used were SwissADME (<http://swissadme.ch/>), pkCSM (<http://biosig.unimelb.edu.au/pkcsml/>), and ProTox-II (http://tox.charite.de/protox_II/). Microsoft Excel Online (<https://www.microsoft.com/en-us/microsoft-365/free-office-online-for-the-web>; free license) was used for data processing and visualization.

2.2. Ligands Preparation

A total of 62 secondary metabolites were reported to be present in the rhizomes of *B. pandurata* used as test ligands, as shown in Table 1. All test ligands' two-dimensional structures were obtained from PubChem (<https://pubchem.ncbi.nlm.nih.gov/>) and then downloaded in SDF format. Energy minimization was performed using Chem3D with MMFF94 force field for each test ligand. For the HER2 receptor, preparations were also carried out using lapatinib as the reference ligand, using the same procedure as the test ligand.

2.3. Receptors Preparation

Two receptors were used in the docking process, consisting of ER- α (PDB ID 3ERT) and HER2 (PDB ID 3RCD), which were downloaded from the Protein Data Bank website (<https://www.rcsb.org/>). The 3ERT receptors consisted of one chain (A), whereas 3RCD had four chains (A, B, C, and D), with the chains used in both receptors for the docking process being chain A. The co-crystal ligand for the 3ERT receptor was 4-hydroxytamoxifen, which was also used as a reference ligand [20], while for the 3RCD receptor, the co-crystal ligand was TAK-285 [21]. Unlike the 3ERT receptor, TAK-285 was only used in the validation process, while lapatinib was used as a reference ligand. The parts of the receptors that were not used (*e.g.*, water, solvent, unused chains) were then removed and given polar hydrogen as well as charges and saved in .pdbqt format using AutoDockTools 1.5.6.

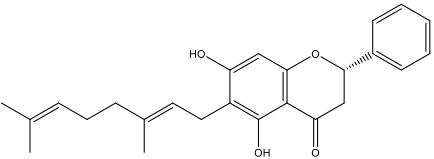
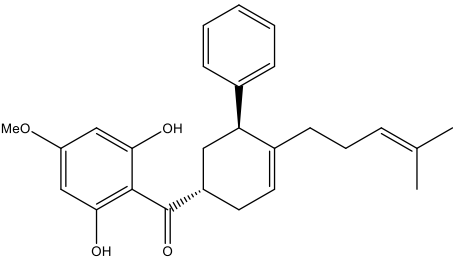
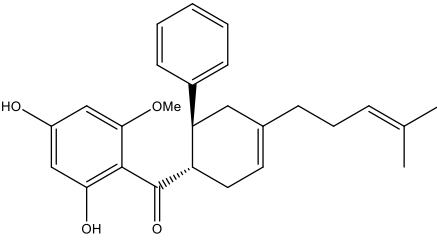
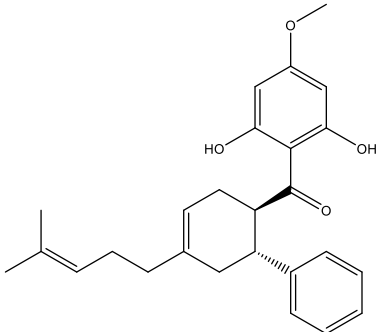
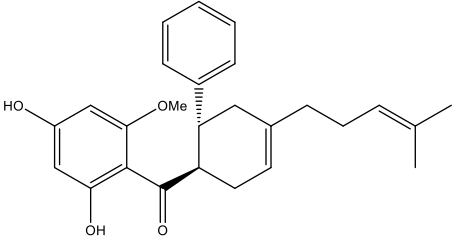
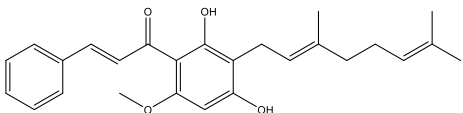
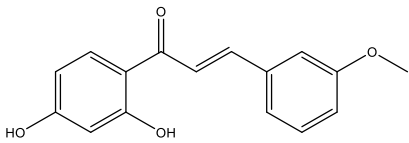
2.4. Validation of Docking Protocol

The docking protocol validation was carried out using the redocking method reported by Morris *et al.* [22]. The observed parameter was a root-mean-square deviation (RMSD), with the maximum limit required not more than 2 Å to conclude that the protocol used was valid and could be used for the docking process. The docking process was repeated three times, then the free energy of binding (ΔG ; kcal/mol) value obtained was calculated using the average value and deviation.

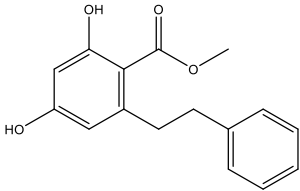
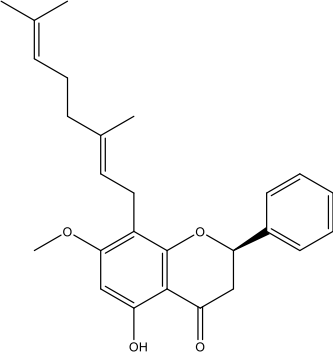
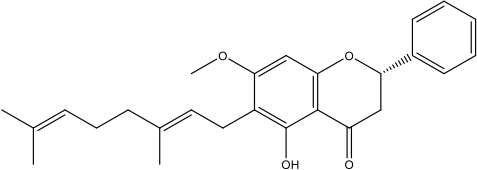
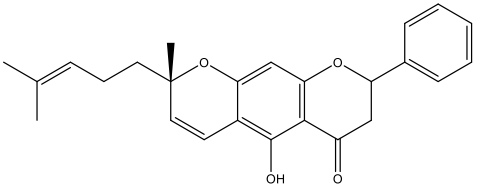
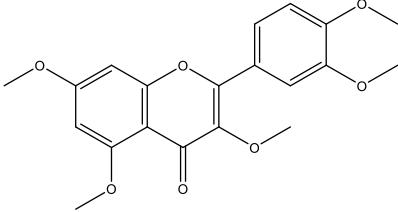
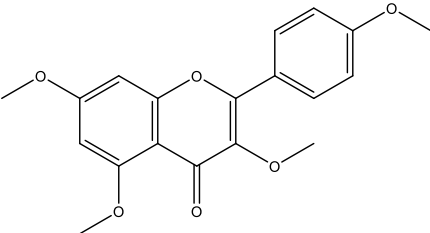
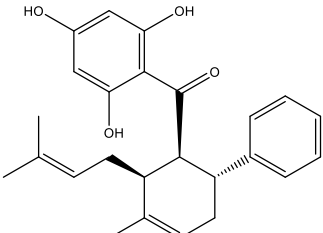
2.5. Molecular Docking

Docking for all test ligands was performed in the same way as the validation process with similar sizes and positions of the grid box for each receptor. The results obtained were grouped into two parameters: ΔG and ligand-receptor

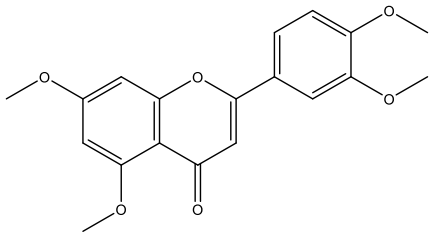
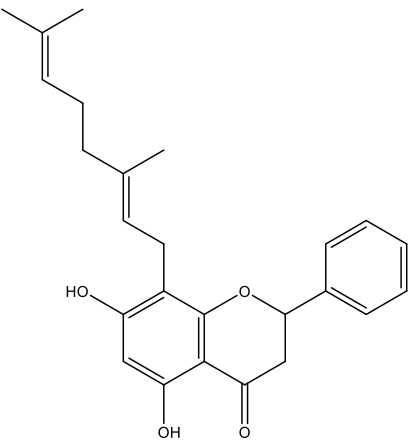
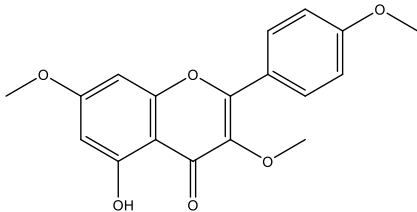
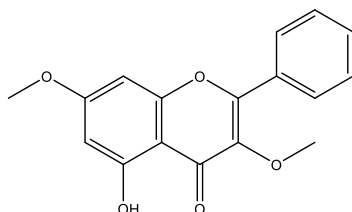
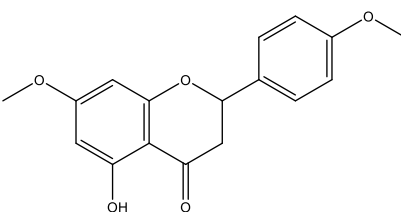
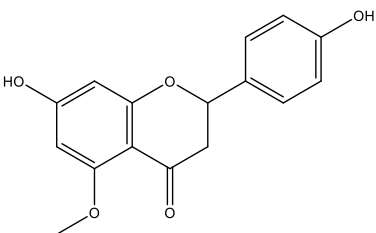
Table 1. The two-dimensional structure of the secondary metabolites of *B. pandurata*.

Compound Number	Name	Two-dimensional Structure	References
1	(-)-6-Geranylpinocembrin		[26]
2	(-)-Krachaizin A		[27]
3	(-)-Krachaizin B		[27]
4	(+)-Krachaizin A		[27]
5	(+)-Krachaizin B		[27]
6	2',4'-Dihydroxy-3'-(1''-geranyl)-6'-methoxychalcone		[26]
7	2',4'-Dihydroxy-3-methoxychalcone		[28]

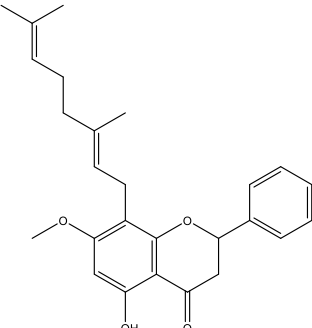
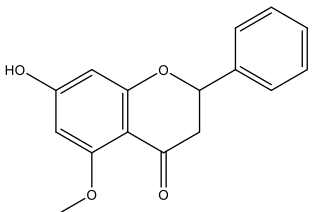
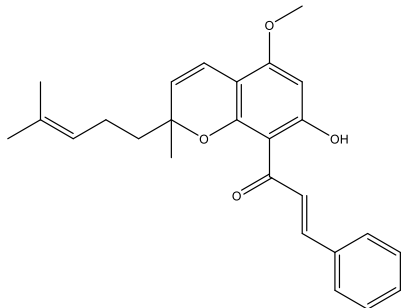
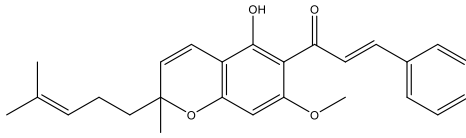
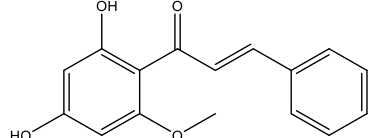
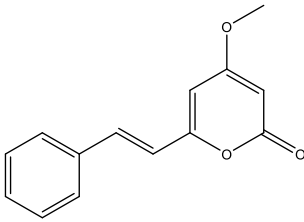
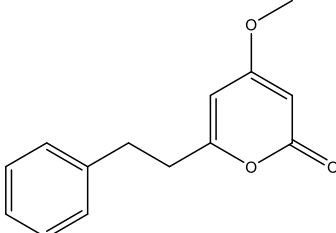
(Table 1) Contd....

Compound Number	Name	Two-dimensional Structure	References
8	2,4-Dihydroxy-6-phenethylbenzoic acid methyl ester		[27]
9	(2R)-8-Geranylpinostrobin		[26]
10	(2S)-6-Geranylpinostrobin		[26]
11	(2S)-7,8-Dihydro-5-hydroxy-2-methyl-2-(4''-methyl-3''-pentenyl)-8-phenyl-2H,6H-benzo(1,2-b-5,4-b')dipyran-6-one		[26]
12	3,5,7,3',4'-Pentamethoxyflavone		[29]
13	3,5,7,4'-Tetramethoxyflavone		[29]
14	4-Hydroxypanduratin A		[30]

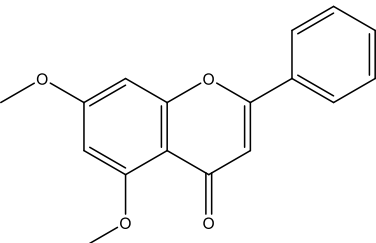
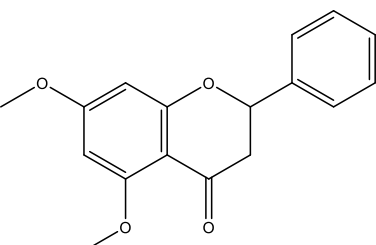
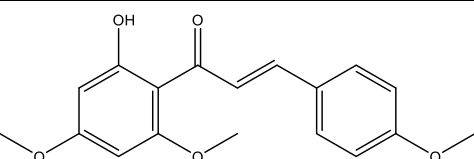
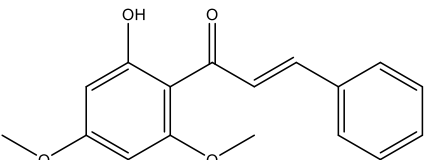
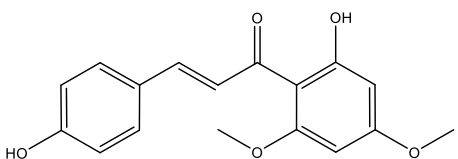
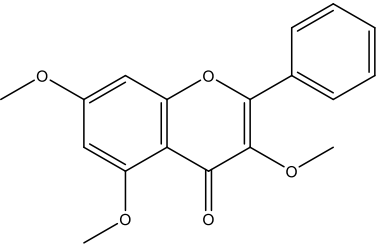
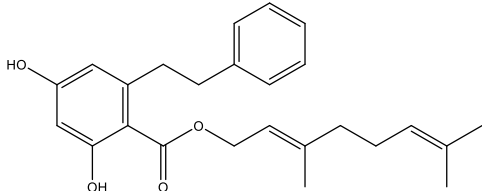
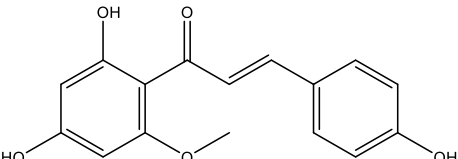
(Table 1) Contd....

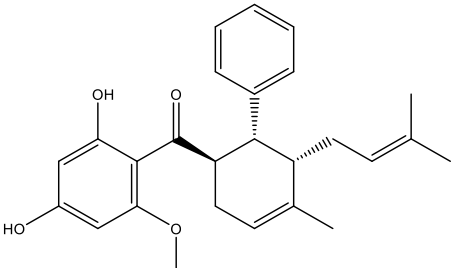
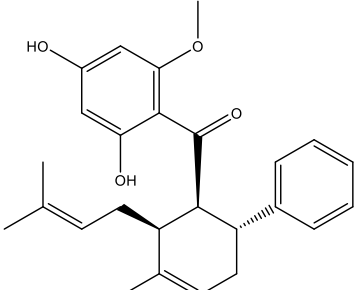
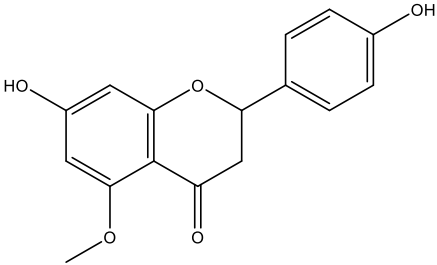
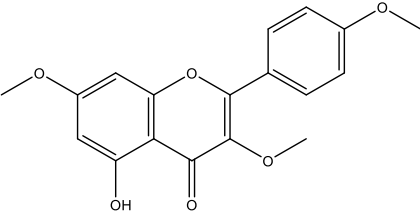
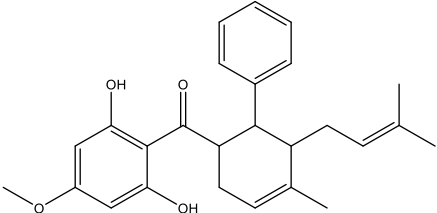
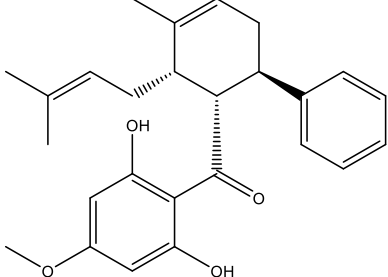
Compound Number	Name	Two-dimensional Structure	References
15	5,7,3',4'-Tetramethoxyflavone		[28]
16	5,7-Dihydroxy-8-geranylflavanone		[27]
17	5-Hydroxy-3,7,4'-trimethoxyflavone		[28]
18	5-Hydroxy-3,7-dimethoxyflavone		[28]
19	5-Hydroxy-4',7-dimethoxyflavanone		[28]
20	7,4'-Dihydroxy-5-methoxyflavanone		[27]

(Table 1) Contd....

Compound Number	Name	Two-dimensional Structure	References
21	7-Methoxy-5-hydroxy-8-geranylflavanone		[27]
22	Alpinetin		[31]
23	Boesenbergin A		[28]
24	Boesenbergin B		[32]
25	Cardamonin		[28]
26	Desmethoxyyangonin		[26]
27	Dihydro-5,6-dehydrokawain		[33]

(Table 1) Contd....

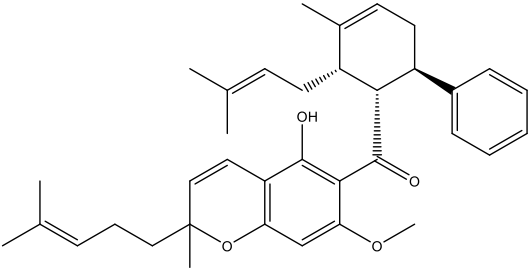
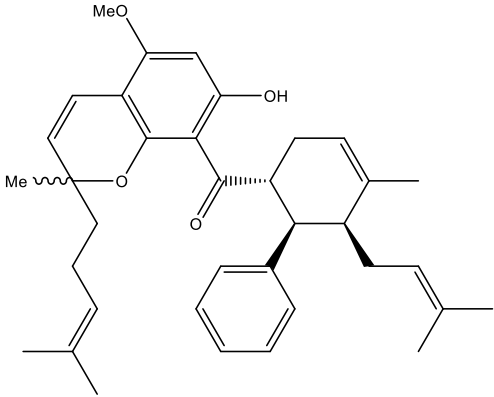
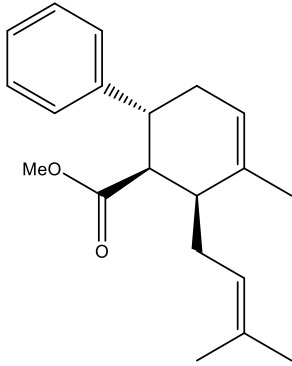
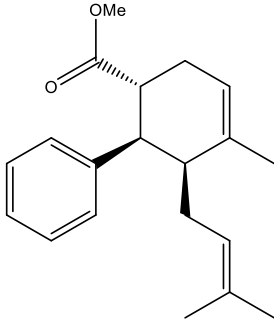
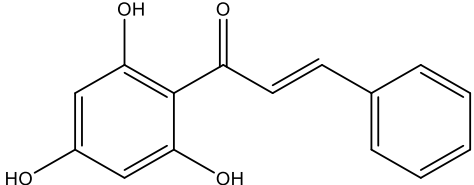
Compound Number	Name	Two-dimensional Structure	References
28	Dimethylchrysin		[28]
29	Dimethylpinocembrin		[28]
30	Flavokawain A		[29]
31	Flavokawain B		[29]
32	Flavokawain C		[26]
33	Galangin trimethyl ether		[28]
34	Geranyl-2,4-dihydroxy-6-phenethylbenzoate		[26]
35	Helichrysetin		[34]

Compound Number	Name	Two-dimensional Structure	References
36	Isopanduratin A1		[26]
37	Isopanduratin A2		[26]
38	Isosakurametin		[26]
39	Kaempferol trimethylether		[28]
40	Nicolaioidesin B		[26]
41	Panduratin A		[32]

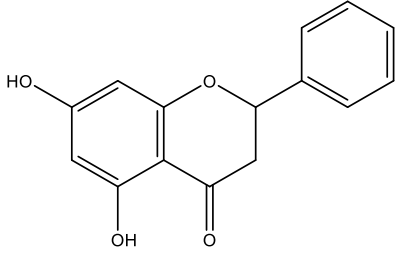
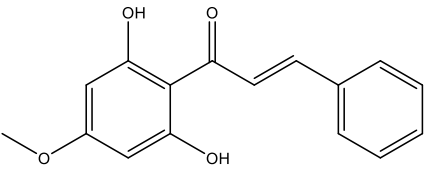
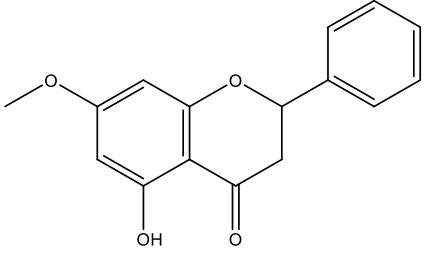
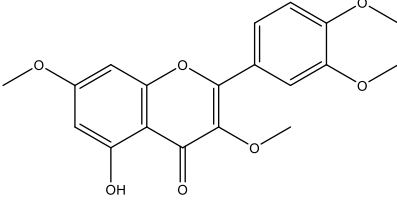
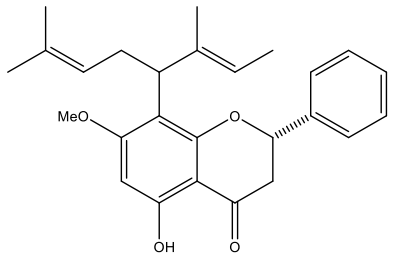
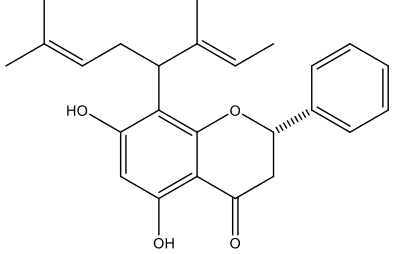
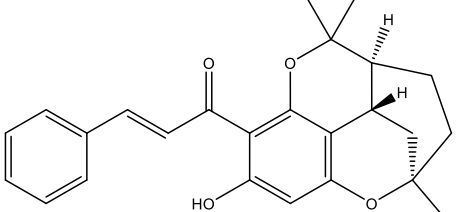
(Table 1) Contd....

Compound Number	Name	Two-dimensional Structure	References
42	Panduratin B		[35]
43	Panduratin C		[34]
44	Panduratin D		[26]
45	Panduratin E		[26]

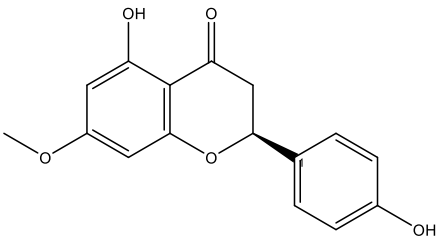
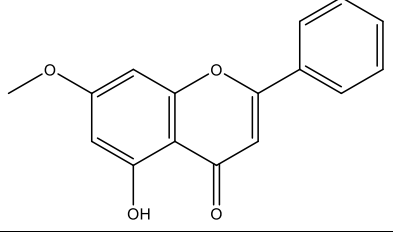
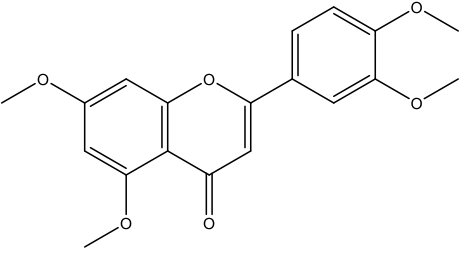
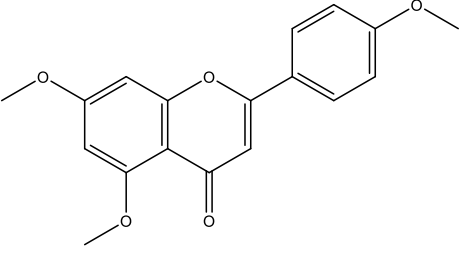
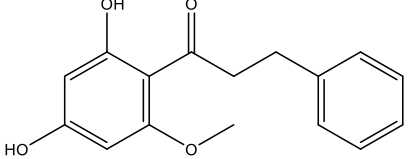
(Table 1) Contd....

Compound Number	Name	Two-dimensional Structure	References
46	Panduratin F		[26]
47	Panduratin G		[26]
48	Panduratin H		[26]
49	Panduratin I		[26]
50	Pinocembrin chalcone		[30]

(Table 1) Contd....

Compound Number	Name	Two-dimensional Structure	References
51	Pinocembrin		[28]
52	Pinostrobin chalcone		[28]
53	Pinostrobin		[28]
54	Retusin		[28]
55	Rotundaflavon I		[27]
56	Rotundaflavon II		[27]
57	Rubranine		[32]

(Table 1) Contd....

Compound Number	Name	Two-dimensional Structure	References
58	Sakuranetin		[33]
59	Tectochrysin		[26]
60	Tetramethoxyluteolin		[28]
61	Trimethylapigenin		[28]
62	Uvangoletin		[34]

interactions, in which ligand-receptor interactions were obtained from the average percentage of the similarity of interactions of the amino acids that interacted and the types of interactions that occurred [23]. As in the validation process, the docking process was also repeated three times. The two parameters of each test ligand were compared for their similarity with 4-hydroxytamoxifen for the 3ERT receptor and lapatinib for the 3RCD receptor, then made in a two-dimensional graph as exemplified in our previous report [23].

2.6. ADMET Prediction

Prediction of each test ligand's ADMET properties was carried out by the steps reported in our previous study [24], which used a combination of more than one ADMET prediction webserver to obtain comprehensive results. The canoni-

cal SMILES format of each test ligand was obtained by conversion using OpenBabel 3.1.1. The prediction results of ADMET properties were then expressed in a graphical form, as illustrated by Sukardiman *et al.* [25].

3. RESULTS

3.1. Validation of Docking Protocol

The RMSD values from the redocking process obtained for the 3ERT and 3RCD receptors were 1.691 and 1.251 Å, respectively. These results indicate that the docking protocol used has met the validity requirements for the docking process. The visualization of ligand overlaid from redocking with the reference ligands from both receptors' crystallographic results is presented in Fig. (1). The redocking ligands show a similar orientation as the crystallographic li-

ands, aside from a slight shift in position. The validation results, along with the docking protocol used, are presented in Table 2. In addition, Table 2 also contains the docking results of lapatinib with the 3RCD receptor, which was used as a reference ligand for that receptor.

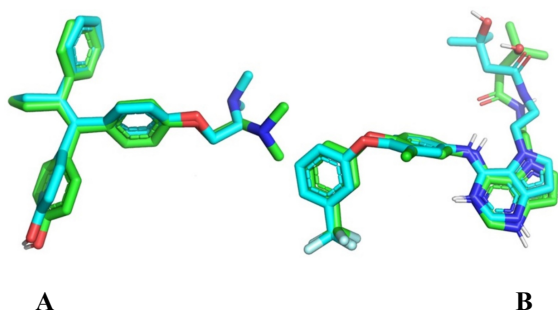


Fig. (1). Overlays of redocking ligands (**blue**) with reference ligands from crystallography data (**green**) at (A) receptors 3ERT with RMSD 1.691 Å and (B) 3RCD with RMSD 1.251 Å. (A higher resolution / colour version of this figure is available in the electronic copy of the article).

The dimensions of the grid box used in the two receptors were relatively small, with dimensions between 22 and 38 Å, adjusting for the co-crystal ligands' size, which was also not too large. The redocking results showed that 22 amino acids interacted with 4-hydroxytamoxifen, while 27 amino acids interacted with TAK-285. The interactions at the 3ERT receptors were predominantly weak interactions, such as the van der Waals interaction but had three hydrogen bonds. The 3RCD receptor showed similar conditions but with many stronger interactions: four hydrogen and four halogen bonds. While lapatinib interacted with 22 amino acids, only 17 amino acids interacted with TAK-285, of which nine had the same type of interactions.

3.2. Molecular Docking

The docking of all test ligands showed varied results, in which no single ligand dominated the two test receptors. Therefore, the best test ligand was determined by considering the two test parameters, both the difference in ΔG value and the percentage of similarity of the ligand-receptor interaction to the reference ligand. The values of these two parameters for all test ligands were then plotted on a two-dimensional graph for a more straightforward observation, as shown in Fig. (2).

The five best test ligands from each receptor were selected from the far left and topmost positions, as shown in Fig. (2). The selected test ligands were compounds **4** ((+)-krachaizin A), **5** ((+)-krachaizin B), **11** ((2S)-7,8-dihydro-5-hydroxy-2-methyl-2-(4''-methyl-3''-pentenyl)-8-phenyl-2H,6H-benzo(1,2-b-5,4-b')dipyran-6-one), **34** (geranyl-2,4-dihydroxy-6-phenethylbenzoate), and **51** (pinocembrin) for the 3ERT receptor and compounds **1** ((-)-6-geranylpinocembrin), **2** ((-)-krachaizin A), **11**, **34**, and **57** (rubranine) for the 3RCD receptor. Two test ligands were ranked in the top five for each receptor, consisting of compounds **11** and **34**. The pattern of the two compounds at the two receptors was similar, in which compound **11** had a smaller ΔG difference with the reference ligand, while com-

pound **34** had a higher percentage of ligand-receptor interaction similarity.

3.3. ADMET Prediction

Prediction of ADMET properties on the three web servers was grouped into five parameters: absorption, distribution, metabolism, excretion, and toxicity. Absorption parameters were obtained from prediction using SwissADME and pkCSM, including implicit Log P (iLOGP), XLOGP3, MLOGP, Silicos-IT Log P, Consensus Log P, ESOL Log S, Ali Log S, Silicos-IT LogSw, Log P, and Water Solubility, as presented in Fig. (3) [36, 37]. Overall, the results obtained indicate that compound **51** had a higher water solubility than the other seven ligands, while the lowest water solubility was shown by compound **34**.

For distribution parameters, the results obtained with pkCSM show variations in several parameters, such as volume of distribution at steady-state (VDss), blood-brain barrier (BBB) permeability, central nervous system (CNS) permeability, and fraction unbound, as presented in Fig. (4). Negative VDss values were shown for compounds **1**, **5**, and **34**. BBB and CNS permeability values were negative with varying ranges, but the lowest values were shown by compound **51**. Overall, all test ligands' distribution profiles were relatively similar, except for compound number **51**, which was predicted to penetrate more easily into BBB and CNS.

For metabolism parameters, the results obtained with SwissADME indicated that all test ligands had potential as inhibitors of cytochrome P450 2C9 (CYP2C9), as presented in Fig. (5). All test ligands also had potential as inhibitors of cytochrome P450 3A4 (CYP3A4), except for compound **34**. Together with compound **51**, compound **34** was also predicted to be a cytochrome P450 1A2 (CYP1A2) inhibitor, in contrast to other ligands. Moreover, compounds **1**, **11**, and **57** were predicted to be cytochrome P450 2C19 inhibitors (CYP2C19). However, only compound **57** had the potential to act as a cytochrome P450 2D6 (CYP2D6) inhibitor among the test ligands. Thus, compound **57** had the most chance as a cytochrome inhibitor with four types of cytochromes.

Only one parameter was observed for the excretion parameters: the total clearance obtained from pkCSM, as shown in Fig. (6). There was a big difference in the total clearance value, in which compounds **57** and **51** only had a total clearance of 0.141 and 0.15 log mL/min/kg, respectively, much lower than the other test ligands. In contrast, the test ligand with the highest total clearance was compound **34** with 1.145 log mL/min/kg, followed by compound **5** with 1.013 log mL/min/kg.

Finally, the toxicity parameters were predicted using ProTox-II with toxicology model parameters for several types of targets and their probabilities, along with the predicted LD₅₀ values, as shown in Fig. (7). As a result, there were two test ligands: compounds **1** and **34**, which did not show a high probability against any toxicity models. For compound **34**, the predicted LD₅₀ value was high (3200 mg/kg), although it was still lower than compound **57** (3800 mg/kg). However, compound **57** had a high probability (0.99) toxicity model for immunotoxicity. The lowest

Table 2. Docking protocol and process validation results.

Parameters	Values		
PDB ID	3ERT	3RCD	
Reference ligand	4-Hydroxytamoxifen	TAK-285	Lapatinib
Grid box size (Å)	38 x 28 x 30	30 x 32 x 22	30 x 32 x 22
Grid box position	x: 30.01 y: -1.913 z: 24.207	x: 12.48 y: 2.964 z: 27.995	x: 12.48 y: 2.964 z: 27.995
RMSD (Å)	1.691	1.251	-
$\Delta G \pm SD$ (kcal/mol)	-9.97 \pm 0.06	-9.8 \pm 0.17	-10.33 \pm 0.06
Amino acid residues	Met-343 ^a Leu-346 ^b Thr-347 ^c Leu-349 ^a Ala-350 ^b Glu-353 ^c Trp-383 ^a Leu-384 ^a Leu-387 ^b Met-388 ^b Leu-391 ^a Arg-394 ^a Phe-404 ^a Glu-419 ^a Gly-420 ^a Met-421 ^b Ile-424 ^a Leu-428 ^b Gly-521 ^a His-524 ^a Leu-525 ^c Met-528 ^a - - - - -	Leu-726 ^a Gly-727 ^a Ser-728 ^a Gly-729 ^a Gly-732 ^a Thr-733 ^a Val-734 ^b Ala-751 ^d Ile-752 ^a Lys-753 ^b Met-774 ^a Ser-783 ^d Arg-784 ^d Leu-785 ^c Leu-796 ^d Val-797 ^a Thr-798 ^c Gln-799 ^c Leu-800 ^a Met-801 ^a Gly-804 ^a Cys-805 ^a Leu-852 ^c Thr-862 ^c Asp-863 ^a Phe-864 ^f Phe-1004 ^a	Leu-726 ^b Gly-727 ^a Phe-731 ^a Val-734 ^a Ala-751 ^b Lys-753 ^b Leu-755 ^b Ser-783 ^a Leu-785 ^a Leu-796 ^d Thr-798 ^a Gln-799 ^c Leu-800 ^a Met-801 ^a Gly-804 ^a Asn-850 ^a Leu-852 ^f Thr-862 ^c Asp-863 ^a Gly-865 ^d Leu-866 ^a Phe-1004 ^f - - - -

^avan der Waals interaction; ^bAlkyl/Pi-alkyl; ^cHydrogen bonds; ^dHalogen bonds; ^ePi-sigma; ^fPi-Pi T-shaped/Pi-Pi stacked/Amide-Pi stacked.

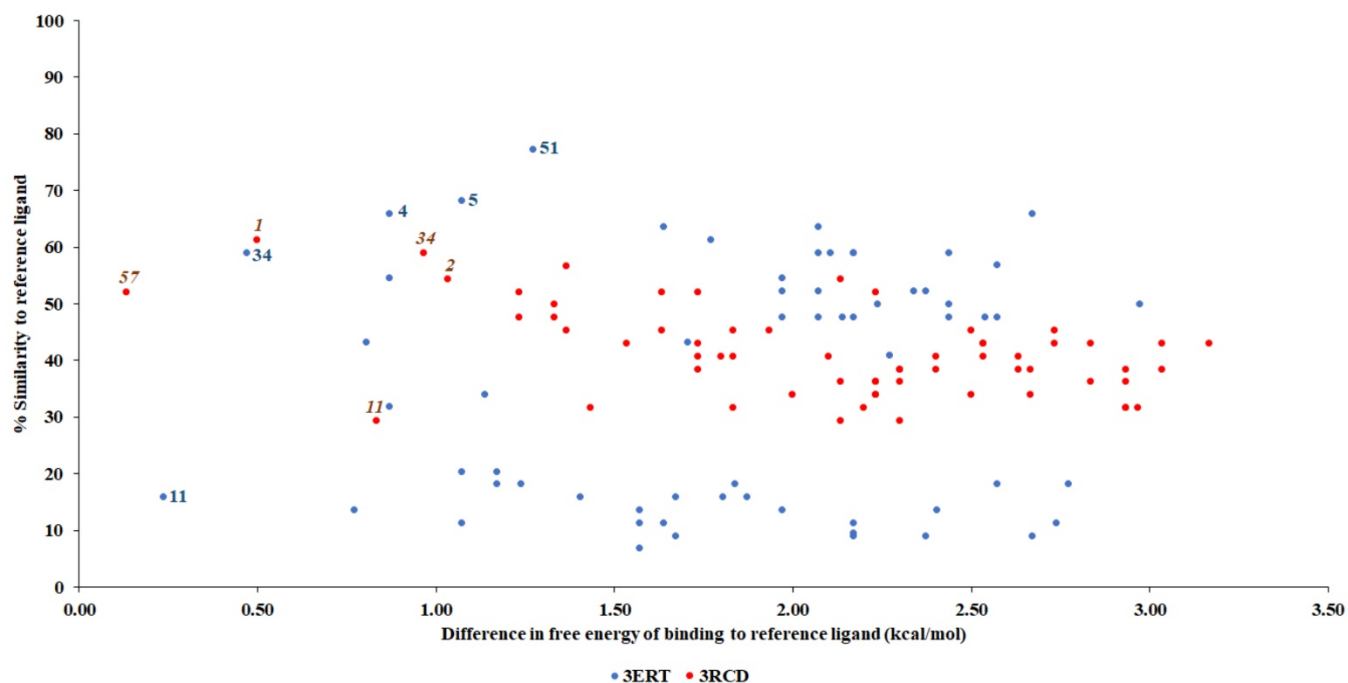


Fig. (2). The two-dimensional graph between the difference in the value of free energy of binding and the percentage of similarity of ligand-receptor interactions compared to the reference ligands on the 3ERT (**blue**) and 3RCD (**red**) receptors. The best five ligands at the far left or topmost position on the graph were selected for each receptor. The five test ligands selected were compounds **4**, **5**, **11**, **34**, and **51** for the 3ERT receptor and compounds **1**, **2**, **11**, **34**, and **57** for the 3RCD receptor. (A higher resolution / colour version of this figure is available in the electronic copy of the article).

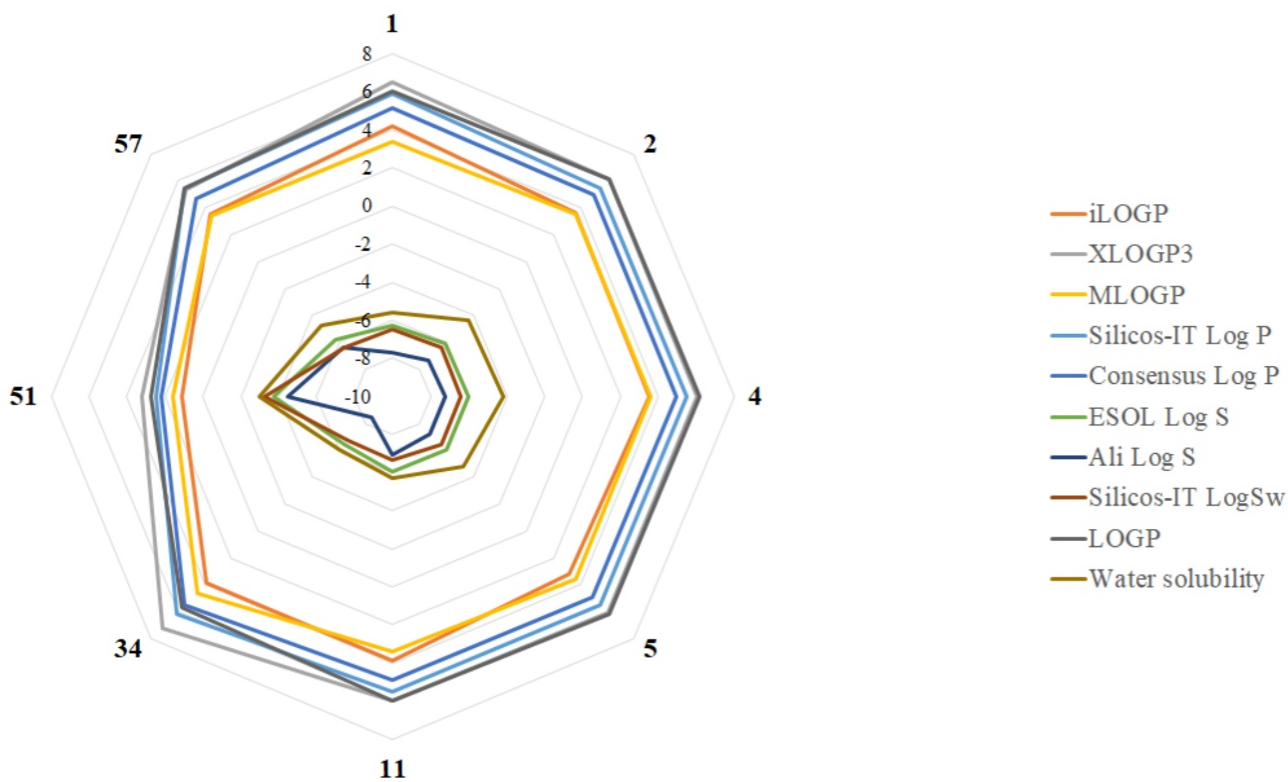


Fig. (3). Prediction of ligand absorption parameters with SwissADME and pkCSM. The highest and lowest predictions of solubility in water were shown by compounds **51** and **34**, respectively. (A higher resolution / colour version of this figure is available in the electronic copy of the article).

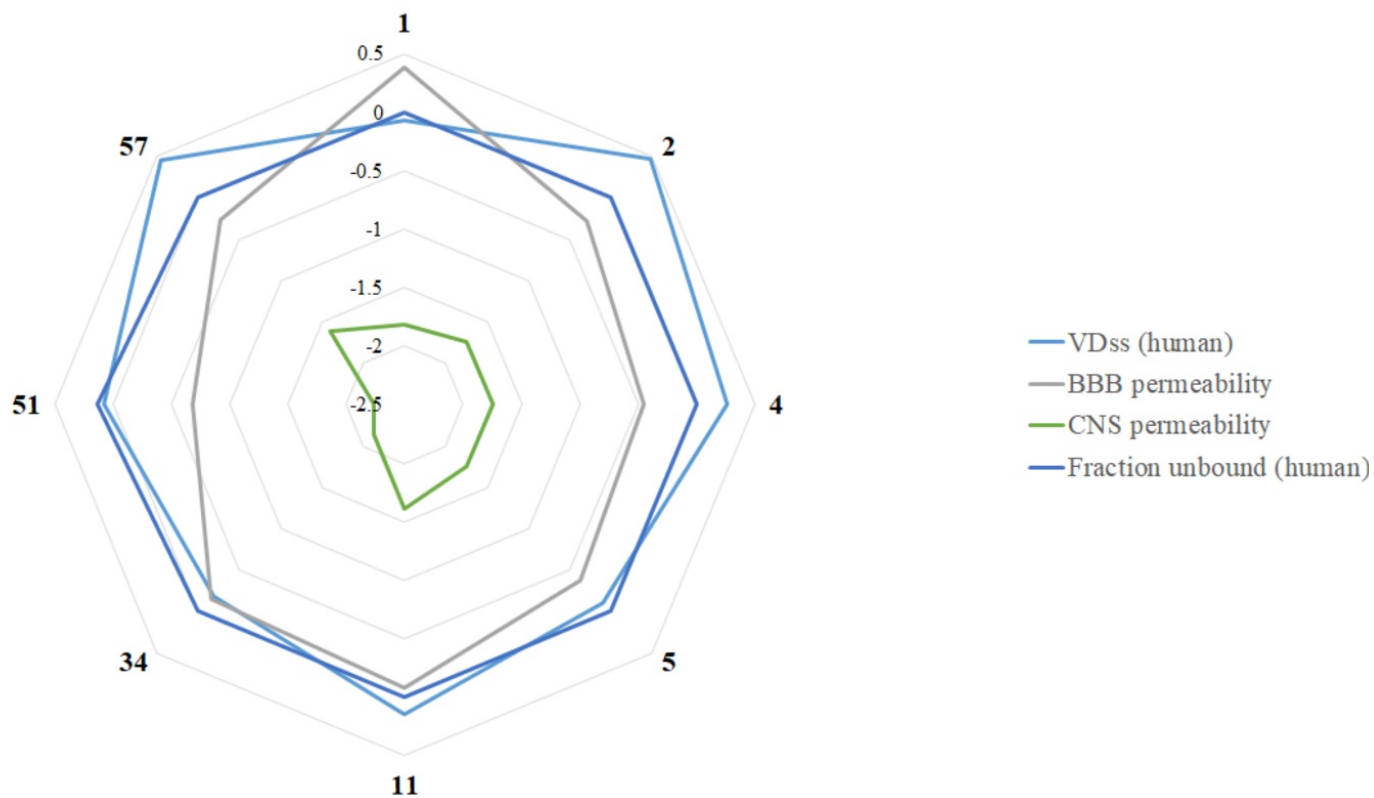


Fig. (4). Prediction of ligand distribution parameters with pkCSM. The test ligand that was predicted to have been the easiest to penetrate to BBB and CNS was compound 51. (A higher resolution / colour version of this figure is available in the electronic copy of the article).

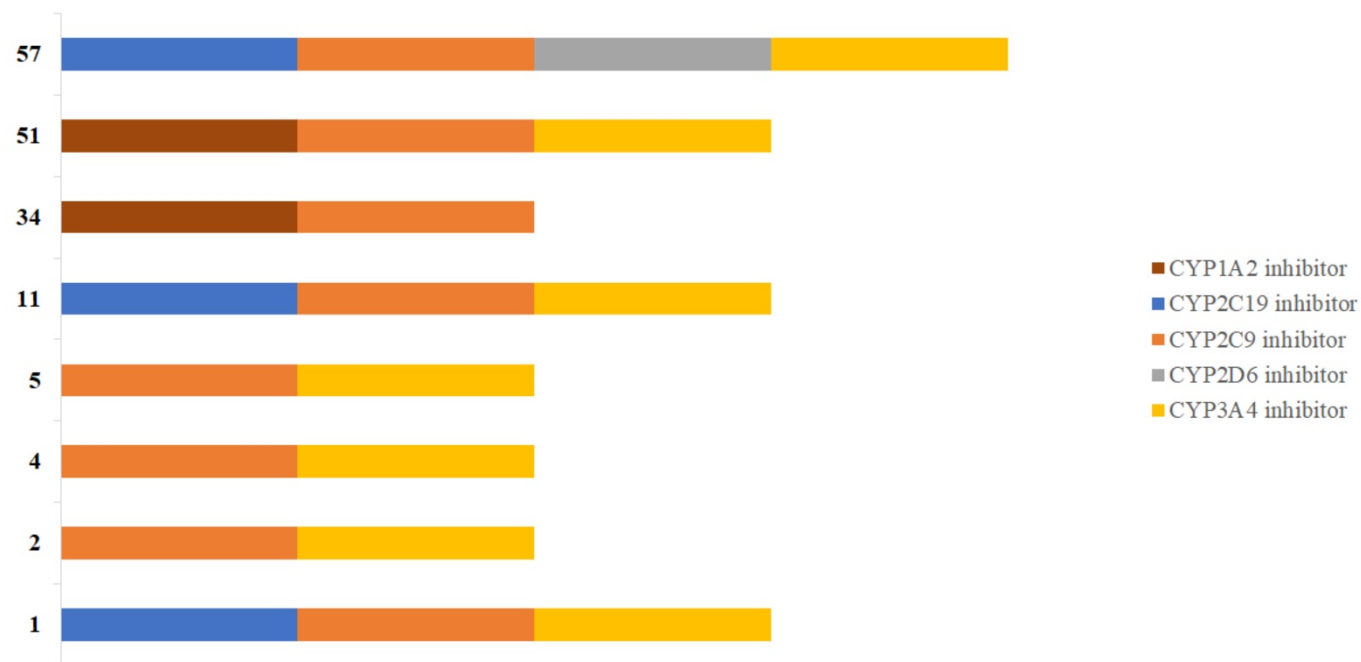


Fig. (5). Prediction of ligand metabolism parameters with SwissADME. Compound 57 had the most chances as a cytochrome inhibitor among other test ligands against four types of cytochromes: CYP2C9, CYP3A4, CYP2C19, and CYP2D6. (A higher resolution / colour version of this figure is available in the electronic copy of the article).

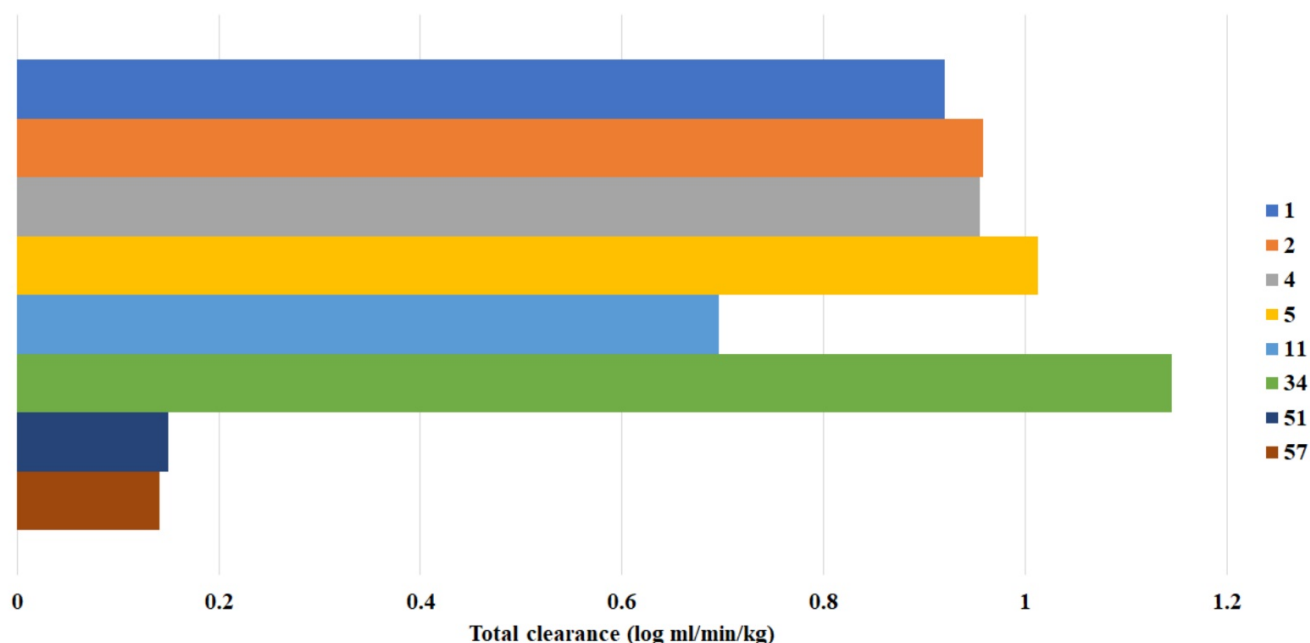


Fig. (6). Prediction of ligand excretion parameters with pkCSM. Compound **57** had the lowest total clearance with 0.141 log mL/min/kg, while the ligand with the highest total clearance was compound **34** with 1.145 log mL/min/kg. (A higher resolution / colour version of this figure is available in the electronic copy of the article).

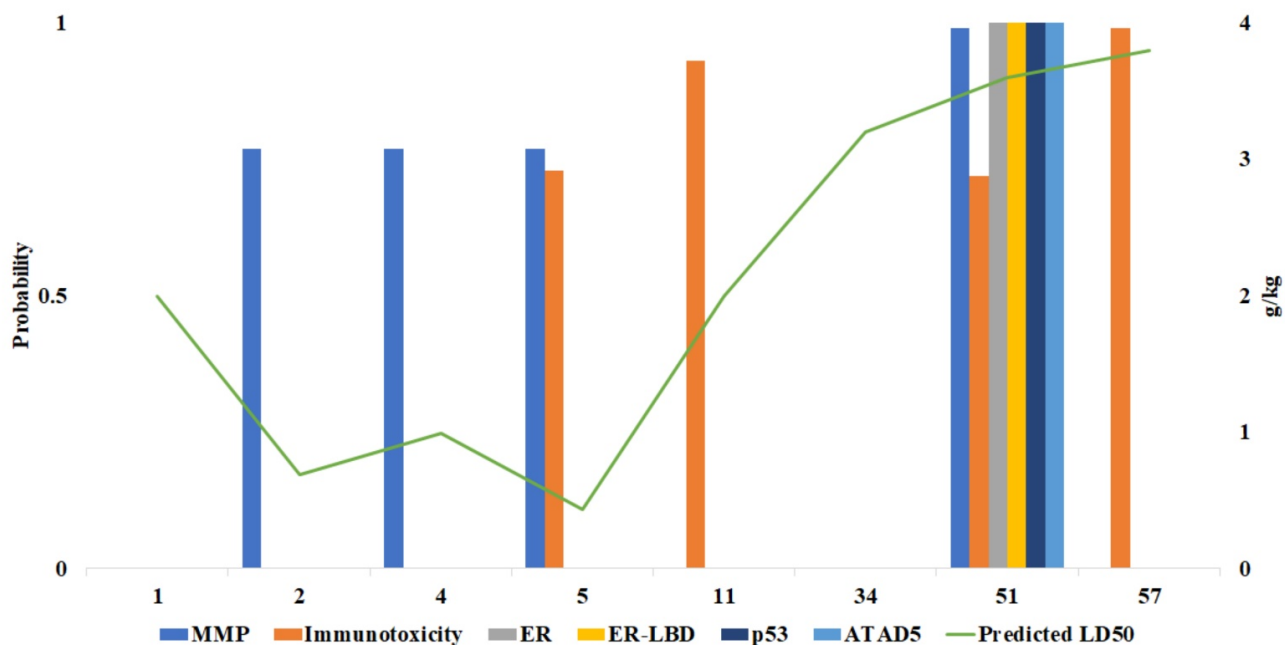


Fig. (7). Prediction of ligand toxicity parameters with ProTox-II. Compound **34** shows a high predicted value of LD₅₀ (3200 mg/kg) without a high probability of toxicity model. Compound **5** shows the lowest predicted value of LD₅₀ with 435 mg/kg, while compound **51** shows a high probability of the toxicity model with the highest number (six targets). (A higher resolution / colour version of this figure is available in the electronic copy of the article).

predicted LD₅₀ for the test ligand was found in compound **5** with 435 mg/kg. While the test ligand with a high probability of toxicity model was shown mainly by compound **51**, with a probability of 0.72, 1.0, 1.0, 0.99, 1.0, and 1.0, respectively, against the target toxicity model for immunotoxicity, estro-

gen receptor α (ER), estrogen receptor ligand-binding domain (ER-LBD), mitochondrial membrane potential (MMP), and phosphoprotein (tumor suppressor) p53 (p53), and ATPase family AAA domain-containing protein 5 (ATAD5).

4. DISCUSSION

Several bioactive compounds from *B. pandurata* have been previously known for their pharmacological activity, especially anticancer properties, such as boesenbergin A against non-small cell lung cancer (A549) cells [38], alpinetin against breast cancer cells 4T1 and MCF-7 [39], and ovarian cancer cells SK-OV-3 [40], cardamonin against PC-3 prostate cancer cells [41], pinostrobin against HeLa cervical cancer cells [15], pinocembrin against HCT 116 colon cancer cells [42] and PC-3 and DU-145 prostate cancer cells [43], as well as panduratin A against breast cancer cells MCF-7, MCF-10A, and T47D [44]. In line with previous studies, the present study also predicted that some metabolites of *B. pandurata* had the potential as ER- α and HER2 inhibitors, including eight metabolites with the highest docking rankings for the two receptors. A combination of current and previous research results indicated that *B. pandurata* might be a good source of natural products which could be developed as anti-breast cancer agents.

Of the eight metabolites, two stand out because they were predicted to have the potential for both ER- α and HER2 receptors: compounds **11** and **34**. The two metabolites reported previously exhibited anticancer activity, as reported in the findings of the study by Win *et al.* [26], confirming their potentials against PANC-1 pancreatic cancer cells. Apart from anticancer properties, these two metabolites were also reported to have other activities, such as anti-inflammatory through TNF- α inhibition [27] and antimicrobials, as summarized by Eng-Chong *et al.* [45]. Still, no previous research declared these two metabolites as ER- α and HER2 inhibitors; therefore, novel findings are discussed in this study.

The choice of ER- α in the development of anti-breast cancer is one of the most commonly used strategies, including ligands derived from natural metabolites. The ER- α crystals that bind to co-crystal ligands, which are selective estrogen receptor modulators/SERMs, such as 4-hydroxytamoxifen (an active metabolite of tamoxifen), are ideal targets in the development of ER- α inhibitors, considering their versatility to act as agonists or antagonists depending on the tissue in which they operate [46]. *In silico* research using this approach has succeeded in identifying potential compounds from various natural metabolites as ER- α inhibitors and then proven *in vitro*, as reported by Pang *et al.* [47]. They reported ER- α inhibitor activity by several metabolites, such as genistein and kaempferol, which validated the feasibility of *in silico* studies for predicting the bioactivities of ligands and provided better insight into the natural products acting as ER- α modulators. Still, the analysis of each metabolite must be carried out carefully, considering the nature of the ER- α that interacts with agonist and antagonist compounds at the same site. This represents one of the main challenges in exploring natural metabolites, in which most of their characteristics are still little known and can lead to adverse effects [48]. Therefore, it is essential to analyze them based on the docking score and compare the interaction against the reference ligand [49]. Another approach that can be used is double docking all test ligands against two receptors, each of which binds to the agonist and antagonist ligands. This approach was reported by Ng *et al.* [50] as a guide to docking with ER- α and has been carried out in

our previous research [18]. However, this approach takes longer with a more complex analysis, considering several ligands have potential both as agonists and antagonists.

In contrast to ER- α , the selection of HER2 as a target in developing an anti-breast cancer agent is slightly more complex, considering that some of the therapies developed for this target are monoclonal antibodies (*e.g.*, trastuzumab, pertuzumab). However, several small molecular inhibitors, such as lapatinib and tucatinib, have also received approval for their use in HER2-positive breast cancer therapy [51]. Despite showing efficacy, these various therapies began to show resistance. Therefore, research on their use with various adjuvant therapies, such as immune checkpoint inhibitors, CDK4/6 inhibitors, and PI3K/AKT/mTOR inhibitors for the treatment of HER2-positive breast cancer, has already started [52]. For natural metabolites, numerous studies have also reported the potential of several compounds, such as ZINC15122021 as HER2 inhibitors, as reported by Li *et al.* [53] and 2-O-caffeoyl tartaric acid, 2-O-feruloyl tartaric acid, and salvianolic acid C as reported by Yang *et al.* [54]. However, *in silico* studies on HER2 require immediate attention because, so far, no receptor crystals have been reported that bind to compounds that have been used in therapy, such as lapatinib. Currently, the most widely used crystals for the development of HER2 inhibitors are those that bind to experimental drugs, such as 2-{2-[4-({5-chloro-6-[3-(trifluoromethyl)phenoxy]pyridin-3-yl)amino]-5h-pyrrolo[3,2-D]pyrimidin-5-yl]ethoxy}ethanol in PDB 3PP0 and TAK-285 in PDB 3RCD, as reported by Shi *et al.* [55] and Yousuf *et al.* [56]. Furthermore, in studies conducted by Li *et al.* [53] and Yang *et al.* [54], lapatinib was used as a reference ligand for these receptors. A similar approach was adopted in this study, in which lapatinib was used as a reference ligand based on the coordinates and dimensions of TAK-285 on the 3RCD receptor. This ensures that the compounds used as references have proven efficacy, thus providing more rational predictions [57].

In this study, apart from molecular docking, an ADMET study was also conducted to determine the metabolites' pharmacokinetic and safety profile with the best docking results. The ADMET study was not carried out on all test ligands, considering that the data obtained from the ADMET study (especially using three types of web servers) would be enormous, and it would be difficult to analyze it. In addition, a good ADMET profile is useless if the test ligand does not have good docking results. Therefore instead of screening, the ADMET study was carried out to support the results of the docking studies, with important information for further *in vitro* and *in vivo* research [58]. The combination of several web servers for the ADMET study was often carried out to obtain more comprehensive information because each web server provides different information, as reported by Vardhan and Sahoo [59] as well as Eswaramoorthy *et al.* [60], which each uses a combination of two web servers. While the combination with three web servers, SwissADME, pkCSM, and ProTox-II, as done in this study, has also been reported by our previous study [24] and then reported again in a study by Rasheed *et al.* [61]. To the best of our knowledge, no other similar studies have reported using more than three web servers simultaneously.

The ADMET studies on compounds **11** and **34** showed mixed results, wherein involving several parameters, compound **11** showed a more favorable profile and vice versa. For example, compound **11** showed a more water-soluble profile than compound **34**. On the other hand, compound **34** showed a relatively less toxic profile than compound **11**. Moreover, compound **34** was relatively unable to penetrate the CNS than compound **11**. However, these two compounds had better ADMET profiles than several other compounds, such as compound **57**, which was predicted to inhibit cytochrome P450s the most and with the smallest total clearance; compound **51**, which showed a high probability of the toxicity model at most, or compound **5** which showed the lowest predicted LD₅₀. Although the prediction of ADMET properties was less than ideal, the other six compounds were still worthy of consideration for further testing because they showed impressive docking results. For example, compound **57**, which exhibited only 0.13 kcal/mol dissimilarity to lapatinib in HER2, or compound **51**, which had 77.27% similarity to 4-hydroxytamoxifen in ER- α . In some cases, the predicted properties of ADMET may differ from the actual conditions, especially for new compounds obtained from natural materials [62, 63].

CONCLUSION

In summary, we found eight metabolites of *B. pandurata* with potential as anti-breast cancer agents, either as ER- α or HER2 inhibitors. Of the eight compounds, compounds **11** and **34** were predicted to have the potential to inhibit both of them, with varying ADMET properties. Our findings also showed that while compound **11** tends to have a docking score closer to the reference ligand, compound **34** shows a higher similarity of ligand-receptor interactions to the reference ligand. However, further *in vitro* and *in vivo* studies are needed to prove the potential and detailed mechanism of the two compounds as anti-breast cancer agents through ER- α or HER2 inhibition.

ETHICS APPROVAL AND CONSENT TO PARTICIPATE

Not applicable.

HUMAN AND ANIMAL RIGHTS

No Animals/Humans were used for studies that are the basis of this research.

CONSENT FOR PUBLICATION

Not applicable.

AVAILABILITY OF DATA AND MATERIALS

The research dataset can be accessed openly at the given website: <https://doi.org/10.5281/zenodo.5508310>.

FUNDING

This work was supported by the Universitas Airlangga under Grant Hibah Riset Mandat 2020 [number

346/UN3/2020]. No potential conflict of interest was reported by the author(s). The funders had no role in the design of the study, data collection, analyses, or interpretation of the data, writing of the manuscript, or decision to publish the results.

CONFLICT OF INTEREST

The authors declare no conflict of interest, financial or otherwise.

ACKNOWLEDGEMENTS

M.R.F.P., H.P., and S.S. participated in the conceptualization. M.R.F.P. and S.S. selected the methodology and software. Validation was done by S.S. Formal analysis was performed by M.R.F.P., E.N.P., D.K., T.W., and S.S. Investigation was done by M.R.F.P., H.P., and S.S. Resources were gathered by S.S. M.R.F.P. and S.S. contributed to data curation. M.R.F.P., E.N.P., D.K., and T.W. participated in writing the original draft. Writing, reviewing, and editing were done by H.P. and S.S. M.R.F.P. contributed to the visualization. Supervision was done by H.P. and S.S. Moreover, H.P. and S.S. contributed to the project administration and funding acquisition. All authors have read and agreed to the published version of the manuscript. The authors would like to thank Dr. Arthur E. Schneider from the Airlangga Writing Consultation Program for providing help in improving the manuscript's readability.

REFERENCES

- [1] Feng, Y.; Spezia, M.; Huang, S.; Yuan, C.; Zeng, Z.; Zhang, L.; Ji, X.; Liu, W.; Huang, B.; Luo, W.; Liu, B.; Lei, Y.; Du, S.; Vuppala-pati, A.; Luu, H.H.; Haydon, R.C.; He, T.-C.; Ren, G. Breast cancer development and progression: Risk factors, cancer stem cells, signaling pathways, genomics, and molecular pathogenesis. *Genes Dis.*, **2018**, *5*(2), 77-106. <http://dx.doi.org/10.1016/j.gendis.2018.05.001> PMID: 30258937
- [2] Krzyszczyk, P.; Acevedo, A.; Davidoff, E.J.; Timmins, L.M.; Marrero-Berrios, I.; Patel, M.; White, C.; Lowe, C.; Sherba, J. J.; Hartmanshenn, C.; O'Neill, K.M.; Balter, M.L.; Fritz, Z.R.; Androulakis, I.P.; Schloss, R.S.; Yarmush, M.L. The growing role of precision and personalized medicine for cancer treatment. *Technology (Singap World. Sci.)*, **2018**, *6*(3-4), 79-100.
- [3] Jean-Quartier, C.; Jeanquartier, F.; Jurisica, I.; Holzinger, A. *In silico* cancer research towards 3R. *BMC Cancer*, **2018**, *18*(1), 408. <http://dx.doi.org/10.1186/s12885-018-4302-0> PMID: 29649981
- [4] Ekins, S.; Mestres, J.; Testa, B. *In silico* pharmacology for drug discovery: methods for virtual ligand screening and profiling. *Br. J. Pharmacol.*, **2007**, *152*(1), 9-20. <http://dx.doi.org/10.1038/sj.bjp.0707305> PMID: 17549047
- [5] Lin, X.; Li, X.; Lin, X. A review on applications of computational methods in drug screening and design. *Molecules*, **2020**, *25*(6), 1375. <http://dx.doi.org/10.3390/molecules25061375> PMID: 32197324
- [6] Yi, F.; Li, L.; Xu, L.-J.; Meng, H.; Dong, Y.-M.; Liu, H.-B.; Xiao, P.-G. *In silico* approach in reveal traditional medicine plants pharmacological material basis. *Chin. Med.*, **2018**, *13*(1), 33. <http://dx.doi.org/10.1186/s13020-018-0190-0> PMID: 29946351
- [7] Narkhede, R.R.; Pise, A.V.; Cheke, R.S.; Shinde, S.D. Recognition of natural products as potential inhibitors of COVID-19 main protease (Mpro): *In-silico* evidences. *Nat. Prod. Bioprospect.*, **2020**, *10*(5), 297-306. <http://dx.doi.org/10.1007/s13659-020-00253-1> PMID: 32557405
- [8] Cragg, G.M.; Pezzuto, J.M. Natural products as a vital source for the discovery of cancer chemotherapeutic and chemopreventive agents. *Med. Princ. Pract.*, **2016**, *25*(Suppl. 2), 41-59. <http://dx.doi.org/10.1159/000443404> PMID: 26679767

- [9] Sung, H.; Ferlay, J.; Siegel, R.L.; Laversanne, M.; Soerjomataram, I.; Jemal, A.; Bray, F. Global Cancer Statistics 2020: GLOBOCAN estimates of incidence and mortality worldwide for 36 cancers in 185 countries. *CA Cancer J. Clin.*, **2021**, *71*(3), 209-249. <http://dx.doi.org/10.3322/caac.21660> PMID: 33538338
- [10] Sun, Y-S.; Zhao, Z.; Yang, Z-N.; Xu, F.; Lu, H-J.; Zhu, Z-Y.; Shi, W.; Jiang, J.; Yao, P-P.; Zhu, H-P. Risk factors and preventions of breast Cancer. *Int. J. Biol. Sci.*, **2017**, *13*(11), 1387-1397. <http://dx.doi.org/10.7150/ijbs.21635> PMID: 29209143
- [11] Falzone, L.; Salomone, S.; Libra, M. Evolution of cancer pharmacological treatments at the turn of the third millennium. *Front. Pharmacol.*, **2018**, *9*, 1300. <http://dx.doi.org/10.3389/fphar.2018.01300> PMID: 30483135
- [12] Meiyanto, E.; Larasati, Y.A. The chemopreventive activity of Indonesia medicinal plants targeting on hallmarks of cancer. *Adv. Pharm. Bull.*, **2019**, *9*(2), 219-230. <http://dx.doi.org/10.15171/apb.2019.025> PMID: 31380247
- [13] Cheah, S-C.; Lai, S-L.; Lee, S-T.; Hadi, A.H.A.; Mustafa, M.R. Panduratin A, a possible inhibitor in metastasized A549 cells through inhibition of NF-kappa B translocation and chemoinvasion. *Molecules*, **2013**, *18*(8), 8764-8778. <http://dx.doi.org/10.3390/molecules18088764> PMID: 23887718
- [14] Yun, J-M.; Kweon, M-H.; Kwon, H.; Hwang, J-K.; Mukhtar, H. Induction of apoptosis and cell cycle arrest by a chalcone panduratin A isolated from *Kaempferia pandurata* in androgen-independent human prostate cancer cells PC3 and DU145. *Carcinogenesis*, **2006**, *27*(7), 1454-1464. <http://dx.doi.org/10.1093/carcin/bgi348> PMID: 16497706
- [15] Jaudan, A.; Sharma, S.; Malek, S.N.A.; Dixit, A. Induction of apoptosis by pinostrobin in human cervical cancer cells: Possible mechanism of action. *PLoS One*, **2018**, *13*(2), e0191523. <http://dx.doi.org/10.1371/journal.pone.0191523> PMID: 29420562
- [16] Le Bail, J.C.; Aubourg, L.; Habrioux, G. Effects of pinostrobin on estrogen metabolism and estrogen receptor transactivation. *Cancer Lett.*, **2000**, *156*(1), 37-44. [http://dx.doi.org/10.1016/S0304-3835\(00\)00435-3](http://dx.doi.org/10.1016/S0304-3835(00)00435-3) PMID: 10840157
- [17] Jones, A.A.; Gehler, S. Acacetin and Pinostrobin inhibit malignant breast epithelial cell adhesion and focal adhesion formation to attenuate cell migration. *Integr. Cancer Ther.*, **2020**, *19*, 1534735420918945. <http://dx.doi.org/10.1177/1534735420918945> PMID: 32493139
- [18] Pratama, M.R.F.; Poerwono, H.; Siswandono, S. Design and molecular docking of novel 5-o-benzoylpinostrobin derivatives as anti-breast cancer. *Thaiphatsachasan*, **2019**, *43*(4), 201-212.
- [19] Youn, K.; Jun, M. Biological evaluation and docking analysis of potent BACE1 inhibitors from *Boesenbergia rotunda*. *Nutrients*, **2019**, *11*(3), 662. <http://dx.doi.org/10.3390/nu11030662> PMID: 30893825
- [20] Shiau, A.K.; Barstad, D.L.; Loria, P.M.; Cheng, L.; Kushner, P.J.; Agard, D.A.; Greene, G.L. The structural basis of estrogen receptor/coactivator recognition and the antagonism of this interaction by tamoxifen. *Cell*, **1998**, *95*(7), 927-937. [http://dx.doi.org/10.1016/S0092-8674\(00\)81717-1](http://dx.doi.org/10.1016/S0092-8674(00)81717-1) PMID: 9875847
- [21] Ishikawa, T.; Seto, M.; Banno, H.; Kawakita, Y.; Oorui, M.; Taniguchi, T.; Ohta, Y.; Tamura, T.; Nakayama, A.; Miki, H.; Kamiguchi, H.; Tanaka, T.; Habuka, N.; Sogabe, S.; Yano, J.; Aertgeerts, K.; Kamiyama, K. Design and synthesis of novel human epidermal growth factor receptor 2 (HER2)/epidermal growth factor receptor (EGFR) dual inhibitors bearing a pyrrolo[3,2-d]pyrimidine scaffold. *J. Med. Chem.*, **2011**, *54*(23), 8030-8050. <http://dx.doi.org/10.1021/jm2008634> PMID: 22003817
- [22] Morris, G.M.; Huey, R.; Lindstrom, W.; Sanner, M.F.; Belew, R.K.; Goodsell, D.S.; Olson, A.J. AutoDock4 and AutoDockTools4: Automated docking with selective receptor flexibility. *J. Comput. Chem.*, **2009**, *30*(16), 2785-2791. <http://dx.doi.org/10.1002/jcc.21256> PMID: 19399780
- [23] Pratama, M.R.F.; Poerwono, H.; Siswodihardjo, S. Introducing a two-dimensional graph of docking score difference vs. similarity of ligand-receptor interactions. *Indones. J. Biotechnol.*, **2021**, *26*(1), 54. <http://dx.doi.org/10.22146/ijbiotech.62194>
- [24] Pratama, M.R.F.; Poerwono, H.; Siswodihardjo, S. ADMET properties of novel 5-O-benzoylpinostrobin derivatives. *J. Basic Clin. Physiol. Pharmacol.*, **2019**, *30*(6), 20190251. <http://dx.doi.org/10.1515/jbpcpp-2019-0251> PMID: 31851612
- [25] Sukardiman, ; Ervina, M.; Fadhil Pratama, M.R.; Poerwono, H.; Siswodihardjo S. The coronavirus disease 2019 main protease inhibitor from *Andrographis paniculata* (Burm. f) Ness. *J. Adv. Pharm. Technol. Res.*, **2020**, *11*(4), 157-162. http://dx.doi.org/10.4103/japtr.JAPTR_84_20 PMID: 33425697
- [26] Win, N.N.; Awale, S.; Esumi, H.; Tezuka, Y.; Kadota, S. Bioactive secondary metabolites from *Boesenbergia pandurata* of Myanmar and their preferential cytotoxicity against human pancreatic cancer PANC-1 cell line in nutrient-deprived medium. *J. Nat. Prod.*, **2007**, *70*(10), 1582-1587. <http://dx.doi.org/10.1021/np070286m> PMID: 17896818
- [27] Morikawa, T.; Funakoshi, K.; Ninomiya, K.; Yasuda, D.; Miyagawa, K.; Matsuda, H.; Yoshikawa, M. Medicinal foodstuffs. XXXIV. Structures of new prenylchalcones and prenylflavanones with TNF-alpha and aminopeptidase N inhibitory activities from *Boesenbergia rotunda*. *Chem. Pharm. Bull. (Tokyo)*, **2008**, *56*(7), 956-962. <http://dx.doi.org/10.1248/cpb.56.956> PMID: 18591809
- [28] Jaipetch, T.; Kanghae, S.; Pancharoen, O.; Patrick, V.; Reutrakul, V.; Tuntiwachwuttikul, P.; White, A. Constituents of *Boesenbergia Pandurata* (Syn. *Kaempferia Pandurata*): Isolation, crystal structure and synthesis of (\pm)-boesenbergin A. *Aust. J. Chem.*, **1982**, *35*(2), 351. <http://dx.doi.org/10.1071/CH9820351>
- [29] Herunsalee, A.; Pancharoen, O.; Tuntiwachwuttikul, P. Further studies of flavonoids of the black rhizomes *Boesenbergia pandurata*. *J. Sci. Soc. Thailand*, **1987**, *13*, 119-122. <http://dx.doi.org/10.2306/scienceasia1513-1874.1987.13.119>
- [30] Trakontivakorn, G.; Nakahara, K.; Shinmoto, H.; Takenaka, M.; Onishi-Kameyama, M.; Ono, H.; Yoshida, M.; Nagata, T.; Tsushida, T. Structural analysis of a novel antimutagenic compound, 4-Hydroxypanduratin A, and the antimutagenic activity of flavonoids in a Thai spice, fingerroot (*Boesenbergia pandurata* Schult.) against mutagenic heterocyclic amines. *J. Agric. Food Chem.*, **2001**, *49*(6), 3046-3050. <http://dx.doi.org/10.1021/jf010016o> PMID: 11410007
- [31] Wangkangwan, W.; Boonkerd, S.; Chavasiri, W.; Sukapirom, K.; Pattanapanyasat, K.; Kongkathip, N.; Miyakawa, T.; Yompakdee, C. Pinostrobin from *Boesenbergia pandurata* is an inhibitor of Ca²⁺-signal-mediated cell-cycle regulation in the yeast *Saccharomyces cerevisiae*. *Biosci. Biotechnol. Biochem.*, **2009**, *73*(7), 1679-1682. <http://dx.doi.org/10.1271/bbb.90114> PMID: 19584530
- [32] Mahidol, C.; Tuntiwachwuttikul, P.; Reutrakul, V.; Taylor, W.C. Constituents of *Boesenbergia Pandurata* (Syn. *Kaempferia Pandurata*). III. Isolation and synthesis of (\pm)-boesenbergin B. *Aust. J. Chem.*, **1984**, *37*(8), 1739. <http://dx.doi.org/10.1071/CH9841739>
- [33] Tuchinda, P.; Reutrakul, V.; Claeson, P.; Pongprayoon, U.; Sema-tong, T.; Santisuk, T.; Taylor, W.C. Anti-inflammatory cyclohex-enyl chalcone derivatives in *Boesenbergia pandurata*. *Phytochemistry*, **2002**, *59*(2), 169-173. [http://dx.doi.org/10.1016/S0031-9422\(01\)00451-4](http://dx.doi.org/10.1016/S0031-9422(01)00451-4) PMID: 11809452
- [34] Cheenpracha, S.; Karalai, C.; Ponglimanont, C.; Subhadhirasakul, S.; Tewtrakul, S. Anti-HIV-1 protease activity of compounds from *Boesenbergia pandurata*. *Bioorg. Med. Chem.*, **2006**, *14*(6), 1710-1714. <http://dx.doi.org/10.1016/j.bmc.2005.10.019> PMID: 16263298
- [35] Pancharoen, O.; Picker, K.; Reutrakul, V.; Taylor, W.C.; Tuntiwachwuttikul, P. Constituents of the Zingiberaceae. X. Diastereomers of [7-Hydroxy-5-Methoxy-2-Methyl-2-(4'-Methylpent-3'-Enyl)-2H-Chromen-8-Yl] [3''-Methyl-2''-(3'''-Methylbut-2'''-Enyl)-6''-Phenylcyclohex-3''-Enyl]M Ethanone (Panduratin B), a constituent of the red rhizomes of a variety of *Boesenbergia pandurata*. *Aust. J. Chem.*, **1987**, *40*(3), 455. <http://dx.doi.org/10.1071/CH9870455>
- [36] Daina, A.; Michielin, O.; Zoete, V. SwissADME: A free web tool to evaluate pharmacokinetics, drug-likeness and medicinal chemistry friendliness of small molecules. *Sci. Rep.*, **2017**, *7*, 42717. <http://dx.doi.org/10.1038/srep42717> PMID: 28256516

- [37] Pires, D.E.V.; Blundell, T.L.; Ascher, D.B. pkCSM: Predicting small-molecule pharmacokinetic and toxicity properties using graph-based signatures. *J. Med. Chem.*, **2015**, *58*(9), 4066-4072. <http://dx.doi.org/10.1021/acs.jmedchem.5b00104> PMID: 25860834
- [38] Isa, N.M.; Abdul, A.B.; Abdelwahab, S.I.; Abdullah, R.; Sukari, M.A.; Kamalidehghan, B.; Hadi, A.H.A.; Mohan, S. Boesenbergin A, a Chalcone from *Boesenbergia rotunda* induces apoptosis via mitochondrial dysregulation and cytochrome c release in a549 cells *in vitro*: Involvement of HSP70 and Bcl2/Bax signalling pathways. *J. Funct. Foods*, **2013**, *5*(1), 87-97. <http://dx.doi.org/10.1016/j.jff.2012.08.008>
- [39] Zhang, T.; Guo, S.; Zhu, X.; Qiu, J.; Deng, G.; Qiu, C. Alpinetin inhibits breast cancer growth by ROS/NF- κ B/HIF-1 α axis. *J. Cell. Mol. Med.*, **2020**, *24*(15), 8430-8440. <http://dx.doi.org/10.1111/jcmm.15371> PMID: 32562470
- [40] Zhao, X.; Guo, X.; Shen, J.; Hua, D. Alpinetin inhibits proliferation and migration of ovarian cancer cells via suppression of STAT3 signaling. *Mol. Med. Rep.*, **2018**, *18*(4), 4030-4036. <http://dx.doi.org/10.3892/mmr.2018.9420> PMID: 30132572
- [41] Pascoal, A.C.R.F.; Ehrenfried, C.A.; Lopez, B.G.-C.; de Araujo, T.M.; Pascoal, V.D.B.; Gilioli, R.; Anhê, G.F.; Ruiz, A.L.T.G.; Carvalho, J.E.; Stefanello, M.E.A.; Salvador, M.J. Antiproliferative activity and induction of apoptosis in PC-3 cells by the chalcone cardamonin from *Campomanesia adamantium* (Myrtaceae) in a bioactivity-guided study. *Molecules*, **2014**, *19*(2), 1843-1855. <http://dx.doi.org/10.3390/molecules19021843> PMID: 24514747
- [42] Kumar, M.A.S.; Nair, M.; Hema, P.S.; Mohan, J.; Santhoshkumar, T.R. Pinoembrin triggers Bax-dependent mitochondrial apoptosis in colon cancer cells. *Mol. Carcinog.*, **2007**, *46*(3), 231-241. <http://dx.doi.org/10.1002/mc.20272> PMID: 17186548
- [43] Chen, Z.; Rasul, A.; Zhao, C.; Millimouno, F.M.; Tsuji, I.; Yamamura, T.; Iqbal, R.; Malhi, M.; Li, X.; Li, J. Antiproliferative and apoptotic effects of pinoembrin in human prostate cancer cells. *Bangladesh J. Pharmacol.*, **2013**, *8*(3), 255-262. <http://dx.doi.org/10.3329/bjp.v8i3.14795>
- [44] Liu, Q.; Cao, Y.; Zhou, P.; Gui, S.; Wu, X.; Xia, Y.; Tu, J. Panduratin A inhibits cell proliferation by inducing G0/G1 phase cell cycle arrest and induces apoptosis in breast cancer cells. *Biomol. Ther. (Seoul)*, **2018**, *26*(3), 328-334. <http://dx.doi.org/10.4062/biomolther.2017.042> PMID: 29301388
- [45] Eng-Chong, T.; Yean-Kee, L.; Chin-Fei, C.; Choon-Han, H.; Sherming, W.; Li-Ping, C.T.; Gen-Teck, F.; Khalid, N.; Abd Rahman, N.; Karsani, S.A.; Othman, S.; Othman, R.; Yusof, R. *Boesenbergia rotunda*: From ethnomedicine to drug discovery. *Evid. Based Complement. Alternat. Med.*, **2012**, *2012*, 473637. <http://dx.doi.org/10.1155/2012/473637> PMID: 23243448
- [46] McDonnell, D.P.; Wardell, S.E. The molecular mechanisms underlying the pharmacological actions of ER modulators: Implications for new drug discovery in breast cancer. *Curr. Opin. Pharmacol.*, **2010**, *10*(6), 620-628. <http://dx.doi.org/10.1016/j.coph.2010.09.007> PMID: 20926342
- [47] Pang, X.; Fu, W.; Wang, J.; Kang, D.; Xu, L.; Zhao, Y.; Liu, A.-L.; Du, G.-H. Identification of estrogen receptor α antagonists from natural products *via in vitro* and *in silico* approaches. *Oxid. Med. Cell. Longev.*, **2018**, *2018*, 6040149. <http://dx.doi.org/10.1155/2018/6040149> PMID: 29861831
- [48] Lecomte, S.; Demay, F.; Ferrière, F.; Pakdel, F. Phytochemicals targeting estrogen receptors: beneficial rather than adverse effects? *Int. J. Mol. Sci.*, **2017**, *18*(7), 1381. <http://dx.doi.org/10.3390/ijms18071381> PMID: 28657580
- [49] Pansar, T.; Poso, A. Binding affinity *via* docking: Fact and fiction. *Molecules*, **2018**, *23*(8), 1899. <http://dx.doi.org/10.3390/molecules23081899> PMID: 30061498
- [50] Ng, H.W.; Zhang, W.; Shu, M.; Luo, H.; Ge, W.; Perkins, R.; Tong, W.; Hong, H. Competitive molecular docking approach for predicting estrogen receptor subtype α agonists and antagonists. *BMC Bioinformatics*, **2014**, *11*(S11), S4. <http://dx.doi.org/10.1186/1471-2105-15-S11-S4>
- [51] Li, S.G.; Li, L. Targeted therapy in HER2-positive breast cancer. *Biomed. Rep.*, **2013**, *1*(4), 499-505. <http://dx.doi.org/10.3892/br.2013.95> PMID: 24648975
- [52] Pernas, S.; Tolaney, S.M. HER2-positive breast cancer: New therapeutic frontiers and overcoming resistance. *Ther. Adv. Med. Oncol.*, **2019**, *11*, 1758835919833519. <http://dx.doi.org/10.1177/1758835919833519> PMID: 30911337
- [53] Li, J.; Wang, H.; Li, J.; Bao, J.; Wu, C. Discovery of a potential HER2 inhibitor from natural products for the treatment of HER2-positive breast cancer. *Int. J. Mol. Sci.*, **2016**, *17*(7), 1055. <http://dx.doi.org/10.3390/ijms17071055> PMID: 27376283
- [54] Yang, S.-C.; Chang, S.-S.; Chen, C.Y.-C. Identifying HER2 inhibitors from natural products database. *PLoS One*, **2011**, *6*(12), e28793. <http://dx.doi.org/10.1371/journal.pone.0028793> PMID: 22174899
- [55] Shi, Z.; Yu, T.; Sun, R.; Wang, S.; Chen, X.-Q.; Cheng, L.-J.; Liu, R. Discovery of novel human epidermal growth factor receptor-2 inhibitors by structure-based virtual screening. *Pharmacogn. Mag.*, **2016**, *12*(46), 139-144. <http://dx.doi.org/10.4103/0973-1296.177912> PMID: 27076751
- [56] Yousuf, Z.; Iman, K.; Iftikhar, N.; Mirza, M.U. Structure-based virtual screening and molecular docking for the identification of potential multi-targeted inhibitors against breast cancer. *Breast Cancer (Dove Med. Press)*, **2017**, *9*, 447-459. <http://dx.doi.org/10.2147/BCTT.S132074> PMID: 28652811
- [57] Meng, X.-Y.; Zhang, H.-X.; Mezei, M.; Cui, M. Molecular docking: A powerful approach for structure-based drug discovery. *Curr. Computeraided Drug Des.*, **2011**, *7*(2), 146-157. <http://dx.doi.org/10.2174/157340911795677602> PMID: 21534921
- [58] Davis, A.M.; Riley, R.J. Predictive ADMET studies, the challenges and the opportunities. *Curr. Opin. Chem. Biol.*, **2004**, *8*(4), 378-386. <http://dx.doi.org/10.1016/j.cbpa.2004.06.005> PMID: 15288247
- [59] Vardhan, S.; Sahoo, S.K. *In silico* ADMET and molecular docking study on searching potential inhibitors from limonoids and triterpenoids for COVID-19. *Comput. Biol. Med.*, **2020**, *124*(103936), 103936. <http://dx.doi.org/10.1016/j.combiomed.2020.103936> PMID: 32738628
- [60] Eswaramoorthy, R.; Hailekiros, H.; Kedir, F.; Endale, M. *In silico* molecular docking, DFT analysis and ADMET studies of carbazole alkaloid and coumarins from roots of *Clausena anisata*: A potent inhibitor for quorum sensing. *Adv. Appl. Bioinform. Chem.*, **2021**, *14*, 13-24. <http://dx.doi.org/10.2147/AABC.S290912> PMID: 33584098
- [61] Rasheed, M.A.; Iqbal, M.N.; Saddick, S.; Ali, I.; Khan, F.S.; Kanwal, S.; Ahmed, D.; Ibrahim, M.; Afzal, U.; Awais, M. Identification of lead compounds against Scm (fms10) in *Enterococcus faecium* using computer aided drug designing. *Life (Basel)*, **2021**, *11*(2), 77. <http://dx.doi.org/10.3390/life11020077> PMID: 33494233
- [62] Gleeson, M.P.; Hersey, A.; Montanari, D.; Overington, J. Probing the links between *in vitro* potency, ADMET and physicochemical parameters. *Nat. Rev. Drug Discov.*, **2011**, *10*(3), 197-208. <http://dx.doi.org/10.1038/nrd3367> PMID: 21358739
- [63] Durán-Iturbide, N.A.; Díaz-Eufracio, B.I.; Medina-Franco, J.L. *In silico* ADME/Tox profiling of natural products: A focus on BIOFACQUIM. *ACS Omega*, **2020**, *5*(26), 16076-16084. <http://dx.doi.org/10.1021/acsomega.0c01581> PMID: 32656429

DISCLAIMER: The above article has been published, as is, ahead-of-print, to provide early visibility but is not the final version. Major publication processes like copyediting, proofing, typesetting and further review are still to be done and may lead to changes in the final published version, if it is eventually published. All legal disclaimers that apply to the final published article also apply to this ahead-of-print version.